Revista de Investigación de Física **14**, 111402102 (2011)

Correlation between superconductivity and structure in the $[Y_{1-x}Pr_x]Ba_2Cu_3O_7$ system

Jesús Flores[1], Angel Bustamante[1], Juan Feijoo[1], J. C. González*[2], Dalbert Sánchez[3] and Geraldo R. C. Cernicchiaro[3]

[1] *Laboratorio de Cerámicos y Nanomateriales, Facultad de Ciencias Físicas, Universidad Nacional Mayor de San Marcos, A.P. 14-0149, Lima 14, Perú*

[2] *Grupo de Investigación de Superficies, Intercaras y Láminas Delgadas, Instituto de Ciencia de Materiales de Sevilla, CSIC, Universidad de Sevilla, Calle Américo Vespucio 49, Isla de la Cartuja, 41092 Sevilla, España*

[3] *Centro Brasileiro de Pesquisas Físicas, Rua Dr. Xavier Sigaud 150, Urca, Rio de Janeiro, Brasil*

Received December 16, 2011 – Accepted January 15, 2012

A structural study of the incorporation of Pr-ion into the Y-site was realized in polycrystalline samples of $[Y_{1-x}Pr_x]Ba_2Cu_3O_7$ through of Rietveld analysis of X-ray diffraction patterns, bond valence method and electronic density diagrams correlating its doping effects on the superconducting properties. The oxygen content was checked by means of μ-Raman spectroscopy, observing the frequency position of O_4-Ag phonon mode, and establishing a relationship among the O_4-Ag mode frequency and the two copper sites, $Cu_{(1)}$ and $Cu_{(2)}$. Two regions are observed with Pr-rich and Y-rich microstructures.
Keywords: Rietveld refinement, Praseodymium doping, superconductivity suppression.

Correlación entre la superconductividad y la estructura en el sistema $[Y_{1-x}Pr_x]Ba_2Cu_3O_7$

Un estudio estructural de la incorporación de iones de Pr en los sítios de Y fue realizado en muestras policristalinas de $[Y_{1-x}Pr_x]Ba_2Cu_3O_7$ a través de: análisis de Rietveld de los patrones de difracción de rayos X, el método de enlaces de valencia y los diagramas de densidad electrónica correlacionando sus efectos del dopaje en las propiedades superconductantes. El contenido de oxígeno fue chequeado por medio de espestroscopia μ-Raman, observando la posición de la frecuencia del modo de fonón de O_4-Ag y estableciendo una relación entre el modo de frecuencia del O_4-Ag y los dos sítios del cobre, $CU_{(1)}$ y $Cu_{(2)}$. Dos regiones microestructurales ricos en Pr e Y han sido observados.
Palabras claves: Refinamiento Rietveld, dopaje de praseodimio, supresión de la superconductividad.

The nature of cuprate oxide superconductors can be elegantly probe by the substitution of Y atom by others Lanthanides entities, $[Y_{1-x}Ln_x]Ba_2Cu_3O_7$ [1,2]. Among these atoms, only Ce, Tb and Pr are not exhibit neither metallic nor superconducting behavior at concentration $x = 1$, with $x_{\text{critical}} \sim 0.50$ [3]. Because the superconducting critical temperature decrease monotonically with increase in Ce, Tb or Pr concentration, and the triple perovskite structure is preserved for the whole range of concentrations x, but among these exceptions $CeBa_2Cu_3O_7$ and $TbBa_2Cu_3O_7$ is not crystalline stable meanwhile $[Y_{1-x}Pr_x]Ba_2Cu_3O_7$ is easily formed in single-phase structure for all Pr content.

The $[Y_{1-x}Pr_x]Ba_2Cu_3O_7$ oxide is a fascinating system because it would sheds lights on the mechanism of superconductivity in cuprate oxide superconductors. Obviously, more information from this kind of system would be extremely useful in order to understand the role played by Pr in this regard [4]. Moreover, the nature of the non-superconducting cuprates has not been fully investigated, although it has been suspected that the absence of superconductivity may have some relationship to the presence of the rare-earth ion in the 4+ state or like other authors claim [5] focus on the importance of the quasi-two dimensional Pr-O-Pr superexchange magnetic coupling through the strong hybridation [6] between the Pr *4f* and the eight O *2p* π-orbitals in the adjacent two CuO_2 layers cannot be

*juanc.gonzalez@icmse.csic.es

ignored because the *4f* wave function is more extended and an anomalously high Neel temperature is observed in $PrBa_2Cu_3O_7$ compound.

On the other hand, the electronic properties in high T_c superconducting compounds are indeed very important because they define the superconducting properties in order to enhance the applicability of these materials [7,8]. The electronic bands states in the electronic structure are very sensitive to short-range order in the atomic positions [5]. Furthermore, the crystallochemical aspects of electronic structure of oxide superconductors are due to the individual properties of constituent ions and also the effect of the atomic substitutions on the electronic properties. We have investigated the $[Y_{1-x}Pr_x]Ba_2Cu_3O_7$ system in some detail to understand the relationship among the oxygen content, crystal structure and magnetic properties, on basis of the results of Rietveld analysis, bond valence method and electronic density diagrams, correlating the results with magnetization measurements and Raman spectra.

Experimental details

Polycrystalline samples of $[Y_{1-x}Pr_x]Ba_2Cu_3O_7$, with x =0, 0.1, 0.3, 0.5 were prepared by standard solid state reaction technique using stoichiometric amounts of high purity powders precursors, such as Y_2O_3, Pr_6O_{11}, $BaCO_3$ and CuO from Alfa Aesear company. The resultant powders were reground and cold pelletized into disc-shape. We applied thermal treatments for three times to improve the homogeneity consisting of the following steps, calcined to 1203 K for 24 h, synthesized to 1208K for 24 h, and then annealed to 773 K for 20h in oxidizing atmosphere; all of them slowly cooled to room temperature.

X-ray powder diffraction data were collected at room temperature with universal powder diffractometer, HGZ (Cu-K_α radiation) in Bragg-Brentano geometry. The diffraction range was between 10° and 80° and step of 0.02°. The standard analyzing program called FullProf was used to perform the Rietveld refinements, bond valence sums and electronic density diagrams. In the Rietveld analysis the background was refined using a fifth-order polynomial equation. A pseudo-Voigt function, a linear combination of Gaussian and Lorentzian ones, was employed to describe the reflection profiles. No absorption or microabsorption corrections were applied to the raw data. The wavelengths of Cu-$K_{\alpha1}$ and Cu-$K_{\alpha2}$ and the intensity ratio were 1.54050 Å, 1.54430 Å and 0.50, respectively. The R's factors and goodness of fitting, S, was used as numerical criteria of fitting. Definitions of R's and S are described in Ref. [9]. To ensure the convergence of the refined parameters, the refinements were carried out according to the following group orders [10]: (1) scale factor, sample displacement, background; (2) cell parameters; (3) peak shape, asymmetry parameter, half width; (4) atomic positions; (5) site occupancies; (6) isotropic thermal parameters.

The μ-Raman spectra were carried out by using a YAG laser (λ = 532 nm) and RH800 Horiba Jovin-Yvon Raman spectrometer with CCD detector cooling by air in back-scattering configuration. The laser power was kept as low as possible (0.5 mW) to avoid deoxygenation of the sample. The magnetization measurements, M(T), was obtained using a magnetic property measurement system (MPMS) with SQUID sensor from Quantum Design in field cooling process with a external field of 5 Oe, for range of temperatures between 5 and 100 K.

Results and Discussion

The X-ray diffraction patterns of $[Y_{1-x}Pr_x]Ba_2Cu_3O_7$ displayed in figure 1, showed a very good crystallinity of the main phase and we also detected very low quantity of the secondary phase $BaCuO_2$, in the order of 2 %.

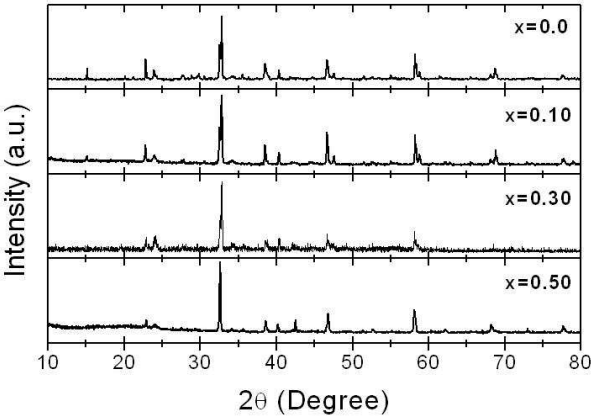

Figura 1: The X-ray diffraction patterns for different concentrations of Pr in $[Y_{1-x}Pr_x]Ba_2Cu_3O_7$ are shown.

The analysis by Rietveld refinement revealed that the crystalline structure stabilized into an orthorhombic phase (Pmmm) for x =0.0, 0.10 and 0.30, but the unit cell increases slightly its symmetry into a tetragonal phase (P4/mmm) for x = 0.5. The change of the unit cell symmetry observed is more pronounced in the *a-axis*, this could be attributed to some oxygen atoms are released out of the structure by doping [11] or as expressed by others authors [12] that exists some kind of disorder in the basal plane of the orthorhombic structure, then due this fact the oxygen atom O(1) and O(5) are slightly moved from its sites (0, 0.5, 0) and (0.5,

0, 0), respectively. On the other hand, it is also possible that the occurrence of either the tetragonal or the orthorhombic structure in samples with similar oxygen stoichiometry can be understood in terms of the relative populations of the O(1) and O(5) sites [13]. Therefore, unequal populations of the O(1) and O(5) sites result in disordered orthorhombic structures; a tetragonal structure results when the O(1) and O(5) populations are equal. In our samples the oxygen content is close to 7, as we will show by Raman measurements with the O(4)-Ag phonon mode frequency denoting well-oxygenated samples.

Pr Content	$x = 0.0$	$x = 0.10$	$x = 0.30$	$x = 0.50$
Unit Cell Symmetry	Pmmm	Pmmm	Pmmm	P4/mmm
Cell parameters (Å)				
a	3.8255	3.8201	3.8419	3.8848
b	3.8871	3.8846	3.8963	3.8848
c/3	3.8873	3.8854	3.8924	3.8831
Volume (Å^3)	173.412	172.971	174.799	175.81
Refined content	0.0	0.06	0.36	0.46
Atomic Positions				
Ba (0.5, 0.5,z)	0.1873	0.1877	0.1889	0.1868
Cu(2) (0, 0, z)	0.3716	0.3658	0.3682	0.3654
O(2)(0.5, 0, z)	0.3932	0.3819	0.3605	0.3671
O(3)(0, 0.5, z)	0.3878	0.3647	0.3659	–
O(4) (0, 0, z)	0.1650	0.1667	0.1614	0.1589
Bond Lenths (Å)				
(Y,Pr)-O(2)	2.308	2.381	2.539	2.484
(Y,Pr)-O(3)	2.322	2.477	2.478	–
Average (Y,Pr)-O(2,3)	2.315	2.429	2.509	–
Distance (Å)				
Cu(2)-Cu(2)	2.9947	3.1285	3.0763	3.1361
Angle (Degree)				
Cu(2)-O(2)-Cu(2)	62.61°	62.60°	56.05°	58.64°
Cu(2)-O(3)-Cu(2)	60.65°	57.89°	57.07°	–
R values(%)				
Rp=	18.4	13.9	31.0	14.1
Rwp=	25.2	18.6	37.1	18.1
Rexp=	12.4	10.2	25.0	10.9
S=	4.11	3.31	2.20	2.77

Tabla 1: Crystallographic parameters

The refined structural parameters are shown in Table 1. As we can seen from the Rietveld refinements results in table 1, the c/3-axis lattice constant increases slightly as the Pr content increases, its value changes from 3.8873 Å ($x = 0$) to 3.8831 Å ($x = 0.5$). This fact it is related with the Shannon radii, which is bigger for Pr^{3+} (1.126 Å) than Y^{3+} (0.96 Å). Thus, a mechanism of hole localization into the superconducting planes is expected due to large valence of Pr compared to Y, but would also suppress the interlayer antiferromagnetic coupling of the CuO_2 superconducting planes. Consequently, we understood that exist a competing mechanisms in the strong chemical pressure in the Pr-site and magnetic coupling between Pr and CuO_2 superconducting planes through the atomic distances among CuO_2-Pr-CuO_2. Although in our results existing deviations in calculating the Pr-O bond length and Y-O length, since we cannot determine precisely the positions of the oxygen atoms by X-ray diffraction, we can only obtain the average bond length. However we can calculate precisely the cation distance between Cu(2)-Cu(2) atoms belonging to two different CuO_2 planes with the Pr-plane between them. Moreover, the angle among the atoms Cu(2)-O(2)-Cu(2) and Cu(2)-O(3)-Cu(2) at the CuO_2 superconducting planes were deeply affected by Pr doping, as it is exhibit in Table 1. Therefore exist a tight

connection between the charge doping level and the lattice parameters in the $[Y_{1-x}Pr_x]Ba_2Cu_3O_7$ structure. Furthermore, Macfarlane *et al* [14], claim that this dependence intensifies on the interplane distances increases when the charge carrier density decrease for all $[Y_{1-x}Ln_x]Ba_2Cu_3O_7$ compounds, how is our case, no matter how the doping is achieved, either by partial substitution or by oxygenation. In case of $PrBa_2Cu_3O_7$ the continuous depletion of charge carriers has similar effects with charge depletion in other cuprates. The accuracy shown in table 1 is enough for us to understand the differences of structural details among different replacement of Pr-ion into the Y-site.

On the other hand, we tested the possibility of the substitution of Pr into the Y- and Ba-site at the same time, but no improvement of the R values and S was found, on the contrary they were worst. Therefore, it is unreasonable to argue in our samples that there is significant mutual substitution between Pr and Ba ions, i.e., cationic disorder.

Pr Content	$x = 0.0$	$x = 0.1$	$x = 0.3$	$x = 0.5$
Y	2.027	0.732	1.068	0.569
Pr	–	1.929	1.473	0.785
Ba	3.644	0.953	1.256	1.065
Cu(1	1.943	1.887	1.211	1.464
Cu(2)	1.113	1.072	1.068	0.561

Tabla 2: Bond valence sums results.

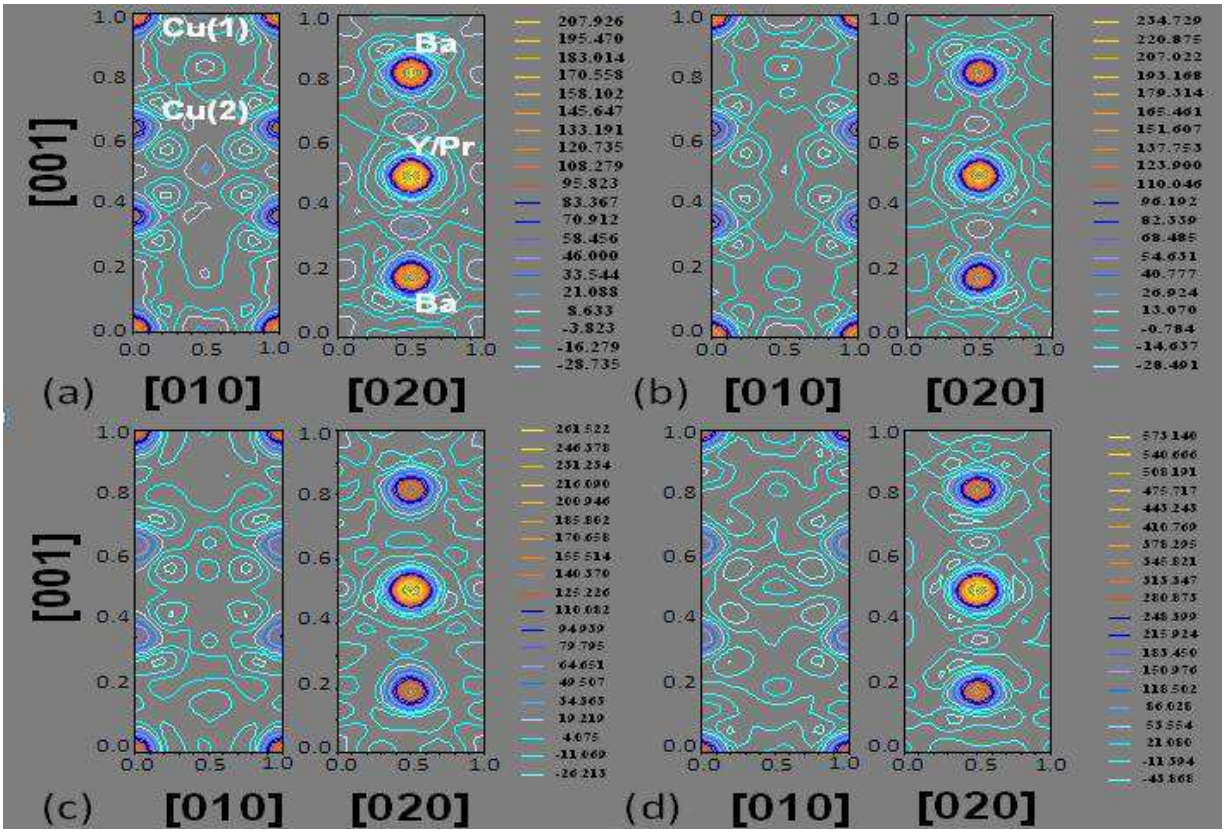

Figura 2: Selected two dimensional electronic density diagrams at two directions [001] [010] and [001] [020] for a) $x = 0.0$, b) $x = 0.10$, c) $x = 0.30$ and d) $x = 0.50$.

In the early studies of the structure of $YBa_2Cu_3O_7$, many authors obtained the quantity of oxygen atoms to be close to 7 [15]. This fact is clearly intimately related to the valency of the cations in the structure. Therefore, according to the principle of valence equilibrium, we must to expect a mixed valency for copper ($Cu^{II,III}$) atoms. The mixed valence at copper site in any given superconductor may be viewed as involving just two oxidation states. This feature is essential for metallic properties and for superconductivity that the two oxi-

dation states be present on one crystallographic site. We have applied the bond valence sums [16,17] in order to estimate the oxidation state of the cations in all our samples by using the structural data from Table 1. The results of our calculus are displayed on Table 2. It can be seen in Table 2 that the Cu(2) bond valence sums (BVS) is higher in $x = 0.0$ but lower in $x = 0.5$, suggesting that the hole concentration on CuO_2 superconducting planes clearly decreases. So the superconductivity is completely suppressed at $[Y_{0.5}Pr_{0.5}]Ba_2Cu_3O_7$, fact strongly correlated with the magnetic results and the increasing distance between CuO_2 superconducting planes. Also, we know that some deviations exist in calculating the bond valence sums of Pr and Y atoms, since we can only obtain the average bond length of Pr-O bond and Y-O bond. The Pr-O bond is longer than Y-O bond, so the calculated BVS of Y is a little smaller than the real value while that of Pr is a little larger it means that the increasing of Pr-ion content affect the charge carriers in the $Cu(2)O_2$ planes and the charge carriers in the charge reservoirs by decreasing the BVS values at Cu(2) and Ba sites, respectively, as it is expressed in table 2. Therefore, the effect of the superconductivity suppression by Pr becomes stronger in the $[Y_{0.5}Pr_{0.5}]Ba_2Cu_3O_7$ compound.

We have obtained additional information about the charge distribution around the atoms from the knowledge of their electronic density diagrams in order to correlate the cation valency and crystallographic results. Figure 2 shows the selected contour plots of the charge density of the valence electrons for $[Y_{1-x},Pr_x]Ba_2Cu_3O_7$ system in the planes (100) and (200) formed by two directions [001]⊥[010] and [001]⊥[020], respectively. The results depict undoubtedly a high electronic density at Y/Pr-site and a clear lack of contours around them, as we introduce more praseodymium atoms more close are the contour plots indicating that this site is almost completely ionized, but in minor level for Cu(2) and Cu(1) sites. However, this Pr-ion is not completely decoupled from the planes CuO_2 above and below by the low values of the contour plots. It is remarkable the influence of Pr-ion is such way that affect the valence electrons at Cu(2) site denoting by the decreasing of its electron valency levels, if we compare with the contour plots of the Cu(1) site. Also, the presence of the Pr-ion perturbates in short range order the atomic positions of O(2) and O(3) at the superconducting planes. Therefore, there is not a magnetic isolation of the Y-site by the magnetic ion and then it interferes with the charge carriers as we will display in the superconducting properties through the magnetization measurements. Our results are in the way of hybridation of Pr $4f$ orbital, consequently, strong hybridation among Pr $4f$-O $2p$/Cu $3d$ leads to hole-localization plus pair-breaking in the conduction band. Moreover, the contours surrounding the Cu(1) and O ions in the basal plane are not characteristic of ordinary ionic compound, but partly covalent.

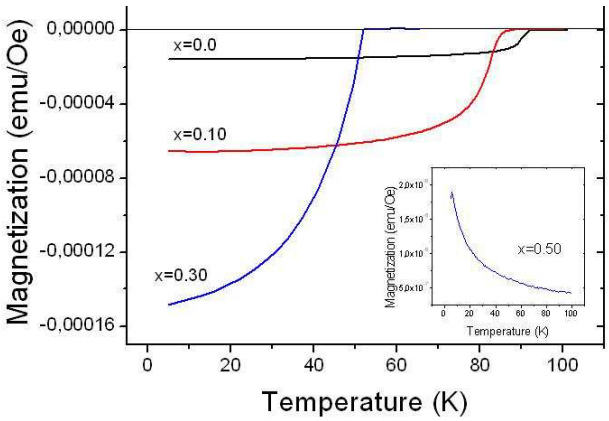

Figura 3: DC magnetization versus temperature.

Figure 3 illustrates the DC magnetization measurements where all Pr cuprates synthesized were found to be superconducting or semiconducting depending on the Pr-content. The $T_{c_{\text{onset}}}$ of the samples varies with the magnetic Pr content, it is seen clearly a sharp drop at the diamagnetic onset temperature. Its decreases from 90 K ($x = 0.0$) to 49 K ($x = 0.3$), meanwhile for $x = 0.5$ the superconductivity is suppressed displaying a paramagnetic behavior. Moreover, a saturation of the diamagnetic signal is observed only in the superconducting samples at low temperatures pointed out the bulk nature of the compounds. On the other hand, we took the following approach that to induce superconductivity is necessary to increase the number of holes per unit cell. As the number of holes increases, the motion of the holes frustrates the *antiferromagnetic* order since the hole hops from site to site without changing the directions of its spin, and thus suppress the *antiferromagnetic* order along its path. Thus, in case of $x = 0.50$ where the distance between Cu(2)-Cu(2) is close to 3.14 Å, the BVS and electronic density for Cu(2) is low, two effects may occur: that Pr causes a strong spin-exchange scattering of the mobile holes and hence suppresses the superconductivity or the extra electrons coming from Pr^{4+} ions fill holes in the CuO_2 planes, and then reduce the positive charge carrier concentration and suppress T_c.

An interesting contribution of Raman spectroscopy in the study of superconductors is the possibility to probe oxygen content of $YBa_2Cu_3O_7$ by the frequency position of the apical oxygen O(4) [18]. The frequency of the O(4)-Ag phonon mode is intimate linked to O(4) oxygen atom in the Barium plane. In our work all the samples were oxygen annealed in an identical way and

its value was found close to 7, therefore we can said that the oxygen content was not disturbed by Pr substitution, so the decreasing of T_c in the samples cannot be attributed to an oxygen deficiency in the structure, then it opens the possibility to argue unequal populations of O(1) and O(5) atoms, clearly correlated with the XRD results. Figure 4(a) shows the Raman spectra for the superconducting samples where we can observe clearly how the frequency of O(4)-Ag phonon mode is very close to 500 cm^{-1}, representing an oxygen content equal to 6.95 ± 0.05 [18].

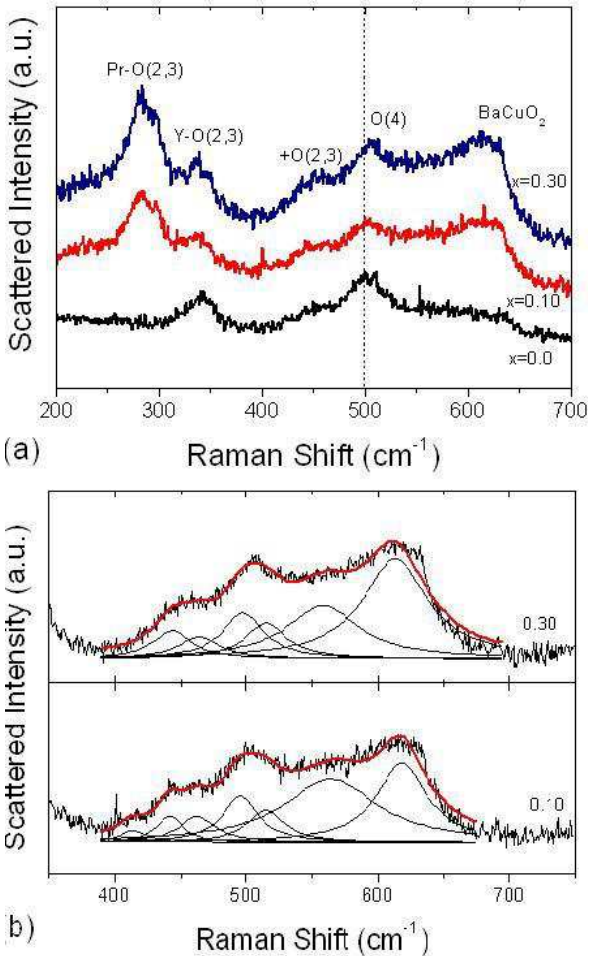

Figura 4: (a) Raman spectra of the superconducting samples, for $x = 0.0$, 0.10 and 0.30; (b) Lorentz fitting curve.

We have deconvoluted the Raman spectra from 380 to 670 cm^{-1} to investigate the underlying phononic spectra by fitting with Lorentzians profiles, as showed in figure 4(b). The frequency of the apical oxygen O(4) vibration shifts up from 501.6 cm^{-1} to 505.3 cm^{-1} as the Pr contents increases up to 30 %. This fact is intimately related to an internal chemical pressure effect due to the substitution of yttrium (0.96 Å) by praseodymium (1.126 Å). Furthermore, this chemical pressure changes the relative interatomic distances between the two copper sites, at the superconducting planes and the chains, additionally the superconducting planes are weakly coupled to the chains by bridging oxygen atom O(4). Thus, must be a clear link between the two copper sites. Borjesson *et al* [19] claim for a relationship between the Raman shift of the O(4)-Ag mode and its relative interatomic distances to the two copper layers, i.e., Cu(2)-O(4) and Cu(1)-O(4), which can be approximated as follows:

$$\omega^2_{O(4)} = \frac{A}{r^3_{Cu(1)-O(4)}} + \frac{B}{r^3_{Cu(2)-O(4)}} \qquad (1)$$

Borjesson *et al* determined the constants A and B from reported changes of the interatomic distances and the O(4) vibration wavenumbers for $[Y_{1-x}Nd_x]Ba_2Cu_3O_7$. In the praseodymium case, we have estimated the value of the A and B constants, from table 1 and figure 4, as $A = 17.41 \times 10^5$ cm^{-2}-Å^3 and $B = 6.61 \times 10^4$ cm^{-2}-Å^3. Moreover, Faulques *et al* [20] explain that the nature of the 580 cm^{-1} broad line appearing is phononic and stems from the oxygen O(1) atoms of Cu(1)O chains. This vibration should be inactive in Raman since the O(1) chain atom is on an inversion center but may be allowed if the crystal symmetry is broken due to crystalline changes. The phonon modes of these atoms in the copper chain layer could be activated in Raman scattering as their site symmetry will be decreased owing to the chain disorder or a better interpretation is if the relative populations of O(1) and O(5) sites are unequal and disordered.

Finally, the appearance of two Raman bands at 280 cm^{-1} and 340 cm^{-1} were pointed as the O(2,3)-B1g phonon mode for $PrBa_2Cu_3O_7$ and $YBa_2Cu_3O_7$, respectively. Zhu [21] has been argued the formation of two regions which are Pr-rich and Y-rich microstructures, separated by boundaries with the Pr-Y connections because in the $[Y_{1-x}Pr_x]Ba_2Cu_3O_7$ system the two end members have different melting points. $PrBa_2Cu_3O_7$ melts at 1253 K, whereas $PrBa_2Cu_3O_7$ melts at 1303 K. There must be some degree of the phase separation $[Y_{1-x}Pr_x]Ba_2Cu_3O_7$ resulting in semiconducting Pr-rich regions and superconducting Y-rich regions. Therefore the Raman spectrum is the superposition of spectra of the coexisting phases.

Summary

The chemical pressure at the Pr-site and the magnetic coupling between Pr and CuO_2 is correlated by the atomic distances among CuO_2-Pr-CuO_2 planes, magnetic properties and oxygen content. It is also pointed

out that Pr doping increased the average Pr-O bond length and the Cu(2)-O-Cu(2) angles within the CuO_2 planes. The Pr-ion doping into the orthorhombic unit cell produce a relative populations of O(1) and O(5) sites unequal and disordered, allowing to the unit cell increases slightly its symmetry into a tetragonal phase and suppressing the superconductivity. Our work support the picture of superconductivity suppression by strong hybridation among Pr *4f*-O *2p*/Cu *3d* leading to hole-localization plus magnetic pair-breaking in the conduction band based on BVS, electronic density plots and magnetization results.

Acknowledgments

This work was supported by the UNMSM and its *Consejo Superior de Investigaciones* under contract N.° 021301101. J. G. thanks to CSIC for his JAE-Doc contract (2009-2012) at the ICMSE-CSIC-US.

Referencias

[1] J. C. Zhang Z. Qin, G. Jin, M. Chen, X. Yao, C. Cai, and S. Cao; J. Phys.: Conf. Ser. **153**, 012039 (2009).

[2] N. R. Rao; J. Solid State Chem.**74**, 147 (1988).

[3] L. Soderholm, K. Zhang, D. G. Hinks, M. A. Beno, J. D. Jorgensen, C. U. Segre, and Ivan K. Schuller; Nature **328**, 604 (1987).

[4] V. Sandu and C. Almansan. Physica C **471**, 133 (2011)

[5] R. Fehrenbacher and T. Rice. Phys. Rev. Lett.**70**, 3471 (1993).

[6] P. Vasek, P. Svodoba, E. Pollert, D. Zemanova, A. Kufudakis, Ch. Mitros, H. Gamari-Seale, and D. Niarchos. Physica C **196**, 94 (1992).

[7] J. Gao, J. L. Sun, and W. H. Tang; IEEE Trans. Appl. Supercond. **11**, 497 (2001).

[8] U. Kabasawa, Y. Tarutani, T. Fukuzawa, N. Sugii, H. Hasegawa, and K. Takagi; J. Appl. Phys. **79**, 7849 (1996).

[9] R. A. Young; The Rietveld Method, Oxford University Press, New York (1996).

[10] J. C. González, D. A. Lándinez, J. Albino Aguiar, and A. Bustamante; Physica C **354**, 375 (2001).

[11] P. Gadaud and B. Kaya; J. Alloys Compounds **211-212**, 296 (1994).

[12] N. Iliev, C. Thomsen, V. Hadjiev, and M. Cardona; Phys. Rev.B **47**, 12341 (1993).

[13] A. K. Ganguli, C. N. R. Rao, A. Sequeira, and H. Rajagopal; Z. Phys. B-Condensed Matter **74**, 215 (1989).

[14] W. Macfarlane, J. Bobroff, P. Mendels, L.Cyrot, H. Alloul, N. Blanchard, G. Collin, and J. Marucco; Phys. Rev. B **66**, 024508 (2002).

[15] J. D. Jorgensen, B. W. Veal, W. K. Kwok, G. W. Crabtree, A. Umezawa, L. J. Nowicki, and A. P. Paulikas; Phys. Rev. B **36**, 5731 (1987).

[16] I. D. Brown and D. Altermatt; Acta Crystallogr. B **41**, 244 (1985).

[17] I. D. Brown; J. Solid State Chem. **90**, 155 (1991).

[18] E. Faulques and S. Lefrant; Cond. Mater. News **5**, 15 (1996).

[19] L. Borjesson, L. V. Hong, M. Kall, M. Kakihana, and P. Berastegui; J. alloys Compd. **195**, 363 (1993).

[20] E. Faulques, P. Mahot, M. Spiesser, T. P. Nguyen, G. Garz, C. Gonzalez, and P. Molinie; Phys. Rev. B **50**, 1209 (1994).

[21] W. J. Zhu, P. Liu, and Z. X. Zhao; Physica C **199**, 285 (1992).